Biochemical and Biophysical Research Communications 606 (2022) 42–48

Contents lists available at ScienceDirect

Biochemical and Biophysical Research Communications

journal homepage: www.elsevier.com/locate/ybbrc

Rho/ROCK mechanosensor in adipocyte stiffness and traction force generation

Tasneem Bouzid [a, 1], Amir Monemian Esfahani [a, 1], Bahareh Tajvidi Safa [a, 1], Eunju Kim [a], Viswanathan Saraswathi [b], Jason K. Kim [c], Ruiguo Yang [a, **], Jung Yul Lim [a, *]

[a] Department of Mechanical and Materials Engineering, University of Nebraska-Lincoln, Lincoln, NE, 68588, USA
[b] Department of Internal Medicine, University of Nebraska Medical Center and VA Nebraska-Western Iowa Health Care System, Omaha, NE, 68105, USA
[c] Program in Molecular Medicine and Division of Endocrinology, Metabolism and Diabetes, Department of Medicine, University of Massachusetts Medical School, Worcester, MA, 01605, USA

ARTICLE INFO

Article history:
Received 8 March 2022
Accepted 15 March 2022
Available online 17 March 2022

Keywords:
Adipocyte
Rho/ROCK
Young's modulus
Traction force
Mechanotransduction

ABSTRACT

It is increasingly recognized that interaction of adipose cells with extracellular mechanophysical milieus may play a role in regulating adipogenesis and differentiated adipocyte function and such interaction can be mediated by the mechanics of adipose cells. We measured the stiffness and traction force of adipose cells and examined the role of Rho/ROCK, the upstream effector of actin cytoskeletal contractility, in affecting these mechanical properties. Cellular Young's modulus obtained from atomic force microscopy (AFM) was significantly reduced by ROCK inhibitor (Y-27632) but elevated by Rho activator (CN01), for both preadipocytes and differentiated adipocytes. Immunofluorescent imaging suggested this could be attributed to the changes in Rho/ROCK-induced stressed actin filament formation. AFM also confirmed that differentiated adipocytes had higher stiffness than preadipocytes. On the other hand, traction force microscopy (TFM) revealed differentiated adipocytes exerted lower traction forces than preadipocytes. Traction forces of both preadipocytes and adipocytes were decreased by ROCK inhibition, but not significantly altered by Rho activation. Notably, an increasing trend of traction force with respect to cell spreading area was detected, and this trend was substantially amplified by Rho activation. Such traction force-cell area correlation was an order-of-magnitude smaller for differentiated adipocytes relative to preadipocytes, potentially due to disrupted force transmission through cytoskeleton-focal adhesion linkage by lipid droplets. Our work provides new data evidencing the Rho/ROCK control in adipose cell mechanics, laying the groundwork for adipocyte mechanotransduction studies on adipogenesis and adipose tissue remodeling.

1. Introduction

Obesity and related metabolic diseases have reached global epidemic proportion [1]. Obesity is characterized by increased adipocyte number (hyperplasia) and size (hypertrophy), which leads to systemic low-grade inflammation and metabolic dysfunction. Revealing the regulatory factors involved in adipogenesis and physiological or pathological adipose tissue remodeling can help better understand obesity and provide methods for obesity prevention and therapy [2]. In addition to biochemical factors, cells and tissues in vivo are exposed to various types and levels of mechanical loading in native environments, and the process of cell sensing and response to these mechanical cues (mechanotransduction) plays a regulatory role in cellular adaptation and homeostasis [3]. Specifically for adipose tissue, it is now recognized that adipocytes are also subjected to compound mechanical loading due to body weight, weight-bearing, and daily motions [4]. Furthermore, mechanical properties of adipocytes, e.g.,

** Corresponding author. W308 Nebraska Hall, Lincoln, NE, 68588, USA.
* Corresponding author. W317.3 Nebraska Hall, Lincoln, NE 68588, USA.
E-mail addresses: ryang6@unl.edu (R. Yang), jlim4@unl.edu (J.Y. Lim).
[1] Contributed equally.

https://doi.org/10.1016/j.bbrc.2022.03.078

cell stiffness [5] and traction force exerted by the cell [6], affect their interactions with extracellular mechanophysical microenvironments, influencing adipogenesis and the functions of mature adipocytes. Here we examined the stiffness and traction force of adipocytes before and after adipogenic differentiation and report, for the first time to our best knowledge, the possible mechanism that governs the changes in adipocyte mechanics.

The mechanotransduction of extracellular loading into intracellular signaling to modulate gene expression, protein synthesis, and downstream behavior is achieved through the actions of mechanosensors. Potential mechanosensors that can be involved in adipogenesis include small GTPase Rho and its downstream effector Rho Kinase (ROCK), as proposed by Hara et al. [7]. They evidenced that obese mice fed a high-fat diet displayed increased ROCK activity in the adipose tissue relative to the control. In general, Rho/ROCK has been established as a crucial regulator of myosin-based cytoskeletal contractility, enabling cells to sense mechanophysical properties of extracellular matrix (ECM) [8–10]. This is achieved via Rho/ROCK induction of stressed actin filaments, followed by enhanced focal adhesion formation (inside-out signaling) or vice versa (outside-in). In obesity, an imbalanced deposition and degradation of ECM components leads to fibrosis around adipocytes, which is associated with increased adipocyte death, inflammation, and insulin resistance [11,12]. However, there is very little understanding on the role of Rho/ROCK in adipocyte sensing of adipose ECM, in either healthy or pathological adipose tissue expansion. Considering Rho/ROCK can be a mechanotransduction mediator of adipogenesis [7], we investigated how Rho/ROCK contributes to the mechanics of preadipocytes and differentiated adipocytes. While studies measured the mechanical properties of adipocytes using atomic force microscope (AFM) and traction force microscope (TFM) [5,6,13,14], mechanosensors that determine the adipocyte mechanical properties have not been identified. Considering cellular mechanics contributes to influence mechano-reactive downstream functions [3], revealing the responsible mechanosensor that affects the stiffness and traction force of adipose cells may lay the groundwork to advance our understanding of the mechanotransduction processes involved in adipogenesis and adipose tissue remodeling.

2. Materials and methods

2.1. Adipogenic cell differentiation

The 3T3-L1 preadipocytes (ATCC, CL-173) were cultured in growth medium composed of high glucose Dulbecco's modified Eagle's medium (DMEM), 10% fetal bovine serum, and 1% penicillin-streptomycin. Adipogenic differentiation was conducted similar to our protocol [15]. Adipogenesis was induced 2 days after seeding by replacing the medium with adipogenic induction medium containing 10 μg/ml insulin, 1 μM dexamethasone, and 0.5 mM 3-isobutyl-1-methylxanthine. After 2 days of induction, the medium was changed to adipogenic maintenance medium with 10 μg/ml insulin. Adipogenic maintenance was continued for 6–7 days until about 90% of cells accumulated lipid droplets. The medium was changed every 2–3 days.

2.2. Inhibitor/activator study

For inhibiting ROCK, cells were treated for 10 min with 0.96 μM of Y-27632 (Selleck) in DMEM, and the medium was replaced with fresh media before mechanics tests. For Rho activation, CN01 (Cytoskeleton Inc.) was dissolved into 20 μl dimethyl sulfoxide and diluted in DMEM at a concentration of 1 unit/ml. Cells were treated with CN01 for 30 min, and the medium was replaced with fresh media before tests.

2.3. Atomic force microscopy

Young's modulus was assessed from the force-displacement curves obtained using a Nanosurf Flex-Axiom AFM device. The AFM setup was equipped on a Zeiss Axio7 inverted microscope and operated with a C3000 controller. To position the AFM probe upon the cell accordingly, the Nanosurf software was utilized. The DNP-10 probe (Bruker Nano) was used having a nominal stiffness and natural frequency of 0.12 N/m and 23 kHz, respectively. The force spectroscopy module with a set point of 5 nN was used. The deflection sensitivity of the probe was assessed on a glass slide before testing cells. Force-displacement curves obtained when the probe approaches the cell were utilized to calculate the Young's modulus with the AtomicJ software (Supplementary Information).

2.4. Traction force microscopy

Traction forces exerted by the cell were measured from the displacements of the fluorescent beads embedded on the cell-seeded gel. The gel with known elastic modulus of 8 kPa (Matrigen) was embedded with 0.2 μm fluorescent beads (Matrigen) at a 1:1600 bead dilution ratio. For differentiated adipocytes, preadipocytes were differentiated on the gel and then used for TFM. The cell-seeded gel was washed with phosphate buffered saline (PBS) and the medium was replaced with phenol red-free DMEM. A Nikon TI-E microscope with a temperature-controllable incubator was used for imaging the cell and fluorescent beads at 20 × magnification. After taking the first set of images, DMEM was replaced by 2 ml trypsin to detach cells, and the gel was relaxed. Then, TRITC image of the beads without cells at the same coordinates was captured. Using ImageJ (NIH) and particle image velocimetry (PIV) plugin, bead displacement fields before and after cell trypsinization were obtained. Bead displacement data were imported to the Fourier Transform Traction Cytometry (FTTC) plugin to construct traction forces based on the gel modulus, following published methods [16]. A custom MATLAB code was used to calculate traction forces (Supplementary Information).

2.5. Immunofluorescent imaging

Cells were fixed for 15 min with 4% formaldehyde solution in PBS. After washing, cells were permeabilized for 5 min with a solution of 0.1% Triton X-100 in PBS, and treated with a 1:100 rhodamine phalloidin (Life Technologies) solution for actin immunostaining. After washing, nuclei were stained with DAPI (Santa Cruz). A Zeiss LSM800 confocal microscope (63 × objective) with ZEN confocal image acquisition and analysis (Zeiss) were utilized.

2.6. Statistics

A one-tailed Student's t-test was conducted to assess the statistical significance of the obtained data compared with the control. Statistics are shown in each figure.

3. Results

3.1. Rho/ROCK-regulated stressed actin filament formation may affect the Young's modulus of preadipocytes and differentiated adipocytes

AFM probing was conducted upon nucleus and cytoplasm for preadipocytes (Fig. 1A) and upon nucleus and lipid droplet for differentiated adipocytes (Fig. 1D). We tried to minimize the effect of substrate rigidity, e.g., AFM probing of cytoplasm region was conducted close to the nucleus. Representative force-displacement

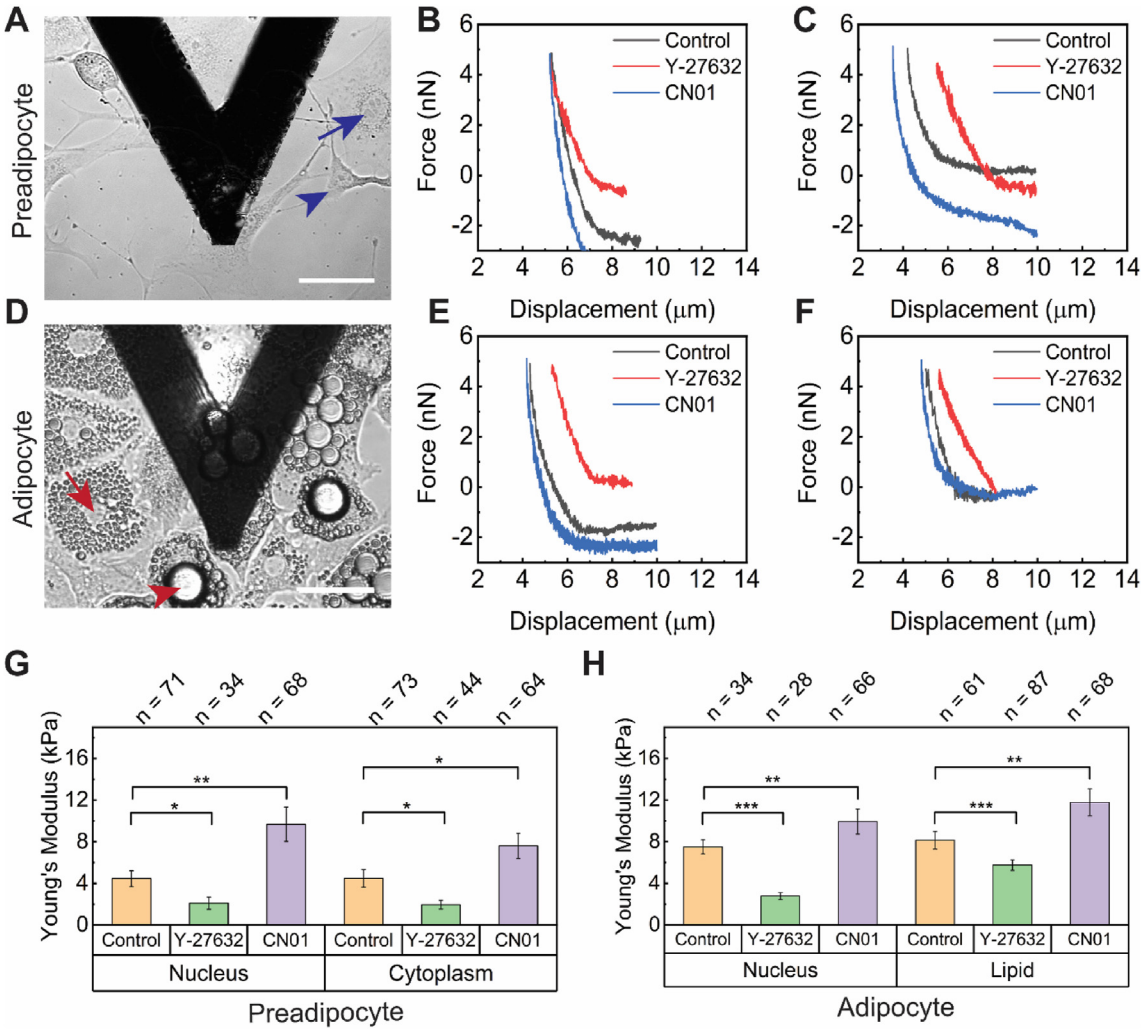

Fig. 1. ROCK inhibition decreases while Rho activation increases Young's modulus of preadipocytes and differentiated adipocytes. **(A)** AFM probe approaching a preadipocyte. Arrow: nucleus; arrowhead: cytoplasm. Representative force-displacement curves of preadipocytes when probing on nucleus **(B)** and cytoplasm **(C)**. ROCK inhibition and Rho activation were conducted using Y-27632 and CN01, respectively. **(D)** AFM probing on differentiated adipocytes. Arrow: nucleus; arrowhead: lipid droplet. Representative force-displacement curves of differentiated adipocytes when probing on nucleus **(E)** and lipid droplet **(F)**. For both preadipocytes **(G)** and differentiated adipocytes **(H)**, ROCK inhibition by Y-27632 decreased while Rho activation by CN01 increased cellular Young's modulus. *: $p < 0.05$, **: $p < 0.01$, and ***: $p < 0.005$ based on repeated AFM probing (n numbers). Scale bar: 20 μm.

curves when the probe approaches the nucleus and cytoplasm of preadipocytes are shown in Fig. 1B and C, respectively. With repeated AFM probing without or with ROCK inhibitor (Y-27632) and Rho activator (CN01) (n numbers, Fig. 1G), we observed ROCK inhibition induced about a two-fold decrease whereas Rho activation resulted in about a two-fold increase in Young's moduli of preadipocytes relative to no inhibitor/activator controls. This was observed for both probing cases upon nucleus and cytoplasm. These suggest that inhibiting Rho/ROCK could prevent stressed actin filament formation, resulting in decreased cell stiffness (see Fig. 2 for actin immunostaining). The exposure to CN01 to activate Rho/ROCK would strengthen actin stress fiber formation leading to an increase in cell stiffness.

Representative AFM curves for differentiated adipocytes are shown in Fig. 1E (probing upon nucleus) and 1F (upon lipid droplets). As in Fig. 1H for differentiated adipocytes, effects of ROCK inhibition by Y-27632 and Rho activation by CN01 on cellular stiffness displayed analogous trends as those for preadipocytes (i.e., ROCK inhibition decreased while Rho activation increased Young's modulus). This was observed similarly when probed upon lipid droplets. These indicate that Rho/ROCK-regulated stressed actin filament formation could also play a vital role in determining the stiffness of differentiated adipocytes. Note, the Young's modulus of differentiated adipocytes was greater than that of preadipocytes (two control cases when probing on nucleus, Fig. 1G and H), consistent with the previous finding that evidenced increased cellular stiffness with the time course of adipogenesis [5].

In immunofluorescent images (Fig. 2), actin filament bundles were seen in preadipocytes and ROCK inhibition by Y-27632 drastically reduced the formation of actin filaments. Exposure to CN01, the Rho activator, produced even stronger stressed actin fibers in preadipocytes. These effects of ROCK inhibitor and Rho activator for preadipocytes were observed similarly for differentiated adipocytes. These results imply the probable involvement of Rho/ROCK-induced stressed actin filaments in determining adipocytic stiffness (Fig. 1). Actin filaments could form cytoskeletal architecture to affect cell stiffness by residing in the cytoplasm and surrounding the nucleus in preadipocytes and surrounding the nucleus and lipid droplets in differentiated adipocytes.

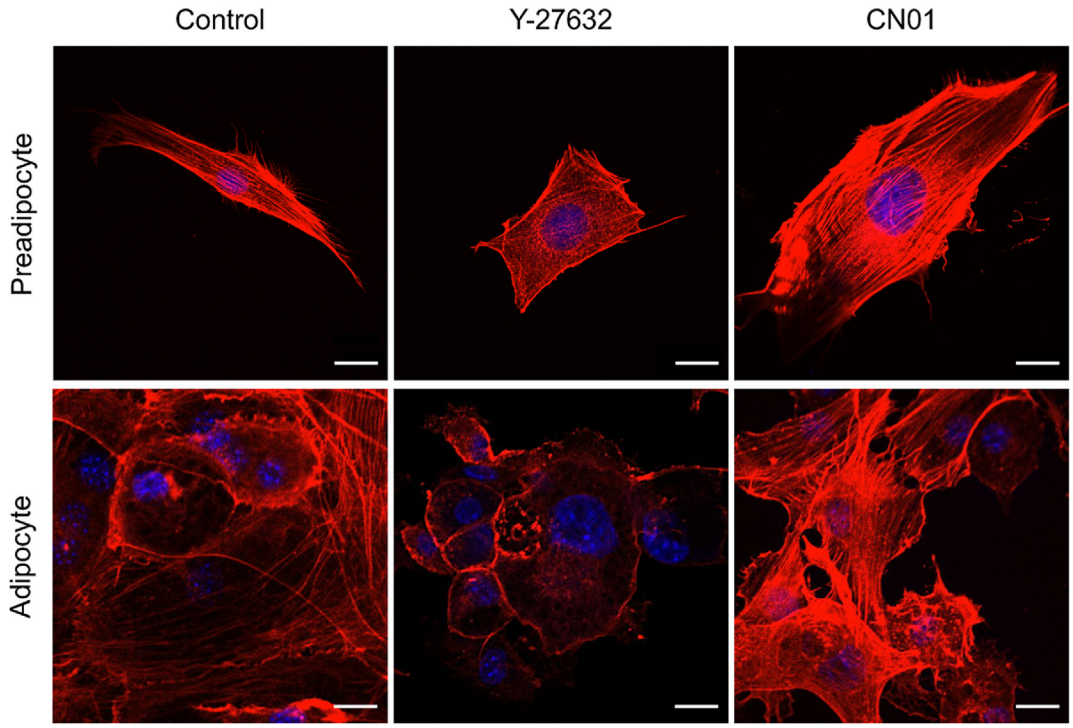

Fig. 2. ROCK inhibitor (Y-27632) disrupts and Rho activator (CN01) strengthens stressed actin filament formation in adipose cells. Actin was immunostained with rhodamine phalloidin and nuclei with DAPI. Scale bar: 20 μm.

3.2. Rho/ROCK affects traction force of adipose cells and traction force dependency on cell spreading area

As another measure of cellular mechanical property, forces exerted by adipose cells were evaluated. Preadipocytes generally had a spindle-shaped morphology, and force vectors from TFM showed that preadipocytes exerted higher forces at focal adhesion sites near filopodia protrusions (red arrows, Fig. 3A–C). With ROCK inhibition by Y-27632, the magnitudes of forces exerted by preadipocytes were distinctly decreased, as seen by the colored force bar with a lowered maximum force (Fig. 3B), force histogram exhibiting a left-side shift or less number of higher force counts (Fig. 3D), and significantly reduced mean traction force averaged throughout each cell (Fig. 3E). Under Rho activation with CN01, some preadipocytes displayed increased traction forces, which however did not reach statistical significance compared with control (Fig. 3E). Thus, the suppression of actin stress fiber formation by ROCK inhibition was effective in reducing cell-exerted force, while Rho activation was less influential in affecting the traction force.

Differentiated adipocytes generally exhibited a rounded shape, and traction forces were distributed rather uniformly throughout cellular area (Fig. 3F–H). The effects of Y-27632 and CN01 on traction forces in differentiated adipocytes, on the other hand, were similar to those observed in preadipocytes. ROCK inhibition induced less counts of high forces (Fig. 3I) and a reduction in average traction force (Fig. 3J), while Rho activation did not result in statistically significant changes (Fig. 3J). Combined, Rho/ROCK may play a mediatory role in affecting the traction force for both preadipocytes and differentiated adipocytes, but with a clearly noticeable result when ROCK was inhibited. Notably, the level of traction forces was markedly lower in differentiated adipocytes compared with preadipocytes (Fig. 3D,E,I,J).

The correlation between traction force and cell spreading area was plotted, as attempted by Abuhattum et al. [6]. Overall, the traction force showed an increasing trend with projected cell area for both preadipocytes (Fig. 3K) and differentiated adipocytes (Fig. 3L). The traction force dependency on cell area was greater when preadipocytes were treated with CN01 resulting in a slope of 3.00×10^{-4} kPa, compared with 1.63×10^{-4} kPa and 1.62×10^{-4} kPa for control and Y-27632 treated preadipocytes, respectively. For differentiated adipocytes, traction forces were lower and cell spreading areas smaller than those of preadipocytes. Though the overall increasing trend could be seen in the magnified view (Fig. 3L), the dependencies for differentiated adipocytes (4.16×10^{-5} kPa for CN01, 1.79×10^{-5} kPa for control, and 1.74×10^{-5} kPa for Y-27632) were an order-of-magnitude lower than those of preadipocytes. Collectively, TFM results indicate that ROCK inhibition decreases traction force and Rho activation increases traction force dependency on cell area, for both preadipocytes and differentiated adipocytes.

4. Discussion

We used AFM and TFM to measure the mechanical properties of 3T3-L1 preadipocytes and differentiated adipocytes under Rho/ROCK inhibition and activation. AFM demonstrated that ROCK inhibition decreases while Rho activation increases cellular stiffness of adipose cells, possibly via the changes of Rho/ROCK-regulated stressed actin filament formation. We also confirmed that differentiated adipocytes exhibit higher cellular stiffness than preadipocytes. On the other hand, TFM showed that differentiated adipocytes exert lower traction forces than preadipocytes. ROCK inhibition reduced traction forces in adipose cells, and while Rho activation did not induce significant changes in traction force magnitude, Rho activation increased the traction force dependency on cell spreading area. The traction force-cell area dependency was substantially lower for differentiated adipocytes. We report, for the first time, the role of a potential mechanosensor, Rho/ROCK, in determining the mechanical properties of adipose cells. Consistent with the notion that mechanophysical interaction of adipose cells

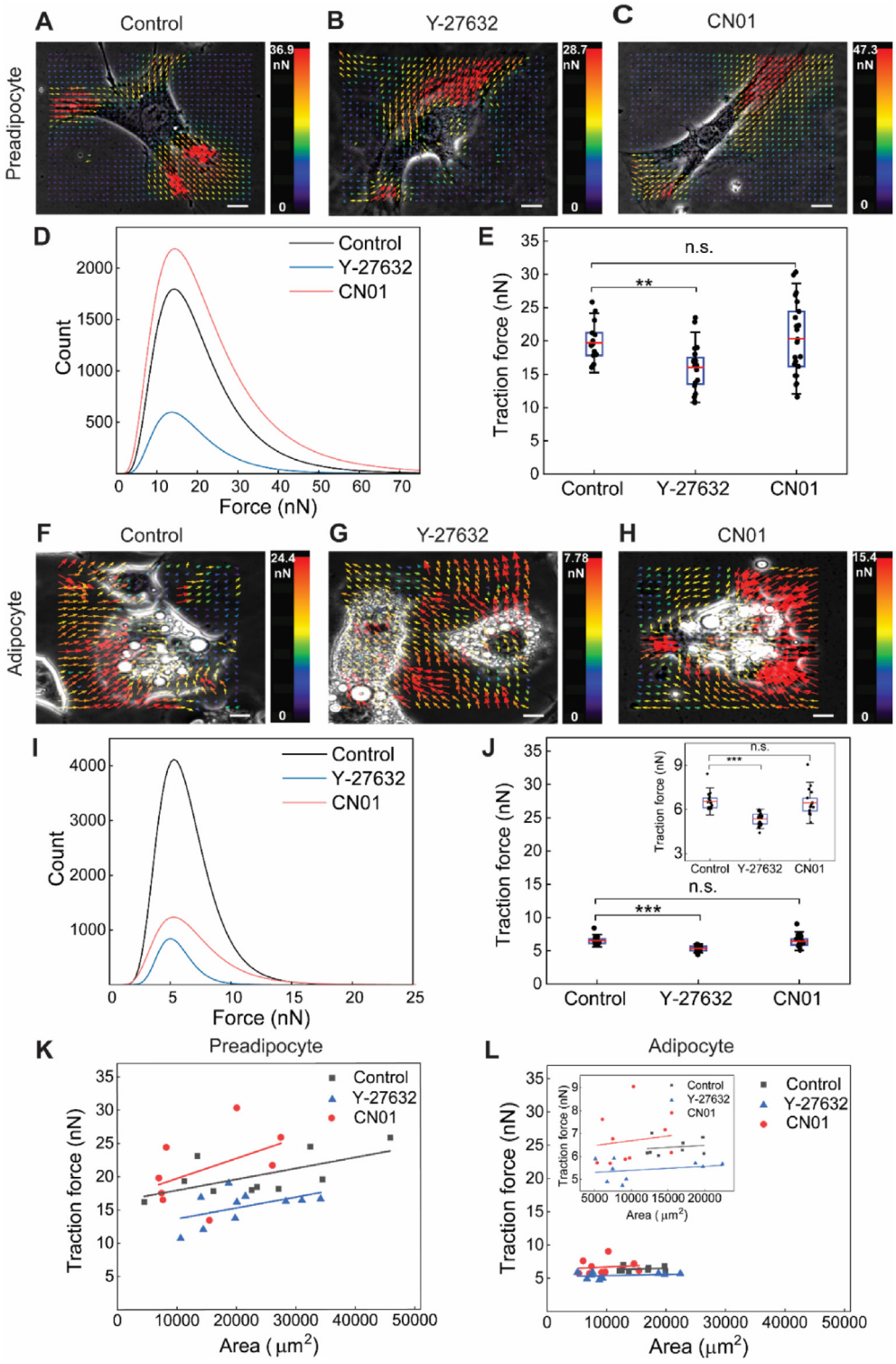

Fig. 3. Traction forces in adipose cells are decreased by ROCK inhibition, and traction force dependency on cell spreading area is increased by Rho activation. **(A–C)** Representative TFM images of preadipocytes from control, Y-27632 treatment, and CN01 treatment, respectively. **(D)** Histogram of traction forces from TFM traction force vectors measured for preadipocytes. **(E)** Average traction force for each cell obtained from entire traction force vectors. ROCK inhibition by Y-27632 significantly decreased traction force in preadipocytes, while Rho activation by CN01 did not induce significant change. **(F–H)** Representative TFM images of differentiated adipocytes. **(I)** Traction force histogram for differentiated adipocytes. **(J)** Differentiated adipocytes displayed substantially lower traction forces than preadipocytes. Trends of Y-27632 and CN01 exposure on the traction force of differentiated adipocytes were similar to those in preadipocytes. **(K,L)** Traction force dependency on projected cell spreading area is increased by Rho activation, and such dependency is less distinct in differentiated adipocytes. **: $p < 0.01$, ***: $p < 0.001$, and n.s.: non-significant. Scale bar: 5 μm.

with extracellular environments may regulate adipogenesis and mature adipocyte function, our findings implicate a potential role of Rho/ROCK in mediating the mechanical adaptation of adipose cells.

Cellular mechanical properties may change throughout the life cycle depending on intracellular functions and extracellular conditions. Mesenchymal stem cells show increased Young's modulus during osteogenesis [17]. Cancer metastatic potential is marked by changes in the mechanical properties of tumorigenic cells, e.g., transformation into invasive cells is associated with decreased cell stiffness [18]. For adipocytes, we showed that differentiated adipocytes have increased Young's modulus relative to preadipocytes (AFM, Fig. 1), in accordance with reported data [5]. It is apparent that mechanical properties of both the cell and the environment alter throughout cell differentiation [19]. For adipocyte differentiation, lipids formed during adipogenesis induce localized changes in tension and compression around lipid droplets, accompanying elevated global cell deformation [20]. Furthermore, pathological expansion of adipocytes within the ECM-confined condition in obesity may evoke mechanical stress to the cells [21]. These changes in intra- and extracellular mechanical environments occurring during adipogenesis, in combination with the observation that lipid droplets are stiffer than cytoplasm based on AFM tests [5], may contribute to the increase in Young's modulus for differentiated adipocytes compared with preadipocytes. Note, the widely used Hertz model was used in extracting the Young's modulus from AFM force-displacement curves (as done in a study by other group [22] and our previous work [23]). It is anticipated that different mechanical models may result in slightly different modulus values, but we do not expect a change in the results of relative comparison among adipocytes of different conditions.

In contrast to cell stiffness assessed from the apical side of the cell by AFM, traction forces measured from the basal side of the cell by TFM decreased for differentiated adipocytes compared with preadipocytes (Fig. 3). During adipogenesis, the cytoskeleton is rearranged to accommodate for the development of lipid droplets [24], which may in turn cause changes in the magnitude and distribution of traction forces. Our traction force results suggest that cytoskeletal rearrangements associated with the lipid droplet formation during adipogenesis may tend to diminish the force transmission capacity through the cytoskeleton-focal adhesion linkage. This may be partly supported by the order-of-magnitude lower traction force-cell spreading area dependency for differentiated adipocytes relative to preadipocytes (Fig. 3K,L), as the increasing trend of traction force with cell area is correlated with an enhanced development of cytoskeleton-focal adhesion architecture.

As a clinically relevant example, the adipose tissue obtained from individuals with type-2 diabetes exhibited a two-fold increase in tissue stiffness compared to that from healthy subjects [25]. During the development of obesity, excessive collagen accumulation in ECM (fibrosis) may lead to decreased tissue plasticity and adipocyte dysfunction. Fibrosis, a typical character of obesity, is responsible for inflammatory response and metabolic impairment [26]. Since adipose tissue expansion accompanies ECM remodeling for adipocytes to accommodate to the new tissue milieu, how adipocytes adapt to external mechanophysical environments could determine healthy or pathological adipose tissue expansion and resultant metabolic responses including insulin resistance [27]. Combined, these highlight the importance of adipose mechanics, related biophysical adaptation, and regulatory mechanosensing mechanism.

It is established for other cells that Rho/ROCK promotes the activity of myosin motor protein, which, in turn, induces stressed actin filament formation and elevates cytoskeletal contractility [28]. This stimulates integrin clustering, enhancing the focal adhesion formation. These steps were attributed as the mechanism of cellular sensing of ECM stiffness and morphology [8–10]. Further, Rho/ROCK-induced changes in cytoskeleton-focal adhesion modulate cell migration [29], proliferation [30], and differentiation [31] for bone, cancer, and stem cells. For adipocytes, Rho/ROCK could play a role in the vicious cycle of obesity [7]: cultured adipocytes displayed lipid accumulation in association with upregulated ROCK and ROCK inhibitor suppressed adipokine secretion during adipogenesis; mice fed a high-fat diet exhibited an increase in ROCK activity and ROCK inhibition alleviated weight gain and insulin resistance for high-fat diet mice. However, this study did not test the role of Rho/ROCK in cell mechanosensing and mechanical properties.

Our results provide evidence that Rho/ROCK may alter adipocyte functioning via formulating the mechanical stiffness inside the cell and the traction force exerted to the matrix. We showed Rho/ROCK manipulates the mechanical properties of adipose cells, not only for preadipocytes with fibroblast-like character but also for differentiated adipocytes. As a trend for differentiated adipocytes, ROCK inhibition decreased cell stiffness and traction force, and Rho activation increased cell stiffness but did not induce a significant change in traction force (Figs. 1 and 3). These trends may be correlated with Rho/ROCK-induced changes in stressed actin filament formation (Fig. 2). The relatively less responsive nature of traction force in differentiated adipocytes was further observed in the traction force-cell area dependency (Fig. 3). Lipid droplets inducing cytoskeletal rearrangements may interrupt force transmission through the cytoskeleton-focal adhesion linkage, even under conditions of enhanced actin filament formation as seen in CN01 treatment, hindering traction force generation at the terminal linkage point of focal adhesion.

Our study is the first to support the implication of Rho/ROCK in the control of preadipocyte and adipocyte stiffness and traction force generation. Further research on the coordination of Rho/ROCK-based actin cytoskeleton with focal adhesion signaling (inside-out and outside-in) and the linker of the nucleoskeleton and cytoskeleton (LINC) may provide additional perspective into the role of these connected mechanosensors in regulating the adipose cell adaptation to extracellular mechanophysical milieus during the process of adjusting adipogenesis and regulating mature adipocyte functions including metabolic responses.

Declaration of competing interest

The authors declare that they have no known competing financial interests or personal relationships that could have appeared to influence the work reported in this paper.

Acknowledgment

Funding supports from National Science Foundation Graduate Research Fellowship (GRFP 1610400, T.B.); Department of Veterans Affairs (V.S.); National Institutes of Health (5U2C-DK093000, J.K.K.); National Science Foundation (1826135; 1936065, R.Y.); National Institute of General Medical Sciences Nebraska Center for Integrated Biomolecular Communication (P20GM113126, R.Y.); Nebraska Collaborative Initiative (R.Y.); National Institute of General Medical Sciences Nebraska Center for the Prevention of Obesity Diseases (P20GM104320, J.Y.L.); and Nebraska Collaborative Initiative (J.Y.L.).

Appendix A. Supplementary data

Supplementary data to this article can be found online at https://doi.org/10.1016/j.bbrc.2022.03.078.

References

[1] M.J. Gurka, S.L. Filipp, M.D. Deboer, Geographical variation in the prevalence of obesity, metabolic syndrome, and diabetes among US adults, Nutr. Diabetes 8 (2018) 1–8, https://doi.org/10.1038/s41387-018-0024-2.

[2] S.S. Choe, J.Y. Huh, I.J. Hwang, et al., Adipose tissue remodeling: its role in energy metabolism and metabolic disorders, Front. Endocrinol. 7 (2016) 30, https://doi.org/10.3389/fendo.2016.00030.

[3] T. Bouzid, E. Kim, B.D. Riehl, et al., The LINC complex, mechanotransduction, and mesenchymal stem cell function and fate, J. Biol. Eng. 13 (2019) 1–12, https://doi.org/10.1186/s13036-019-0197-9.

[4] N. Shoham, A. Gefen, Mechanotransduction in adipocytes, J. Biomech. 45 (2012) 1–8, https://doi.org/10.1016/j.jbiomech.2011.10.023.

[5] N. Shoham, P. Girshovitz, R. Katzengold, et al., Adipocyte stiffness increases with accumulation of lipid droplets, Biophys. J. 106 (2014) 1421–1431, https://doi.org/10.1016/j.bpj.2014.01.045.

[6] S. Abuhattum, A. Gefen, D. Weihs, Ratio of total traction force to projected cell area is preserved in differentiating adipocytes, Integr. Biol. 7 (2015) 1212–1217, https://doi.org/10.1039/C5IB00056D.

[7] Y. Hara, S. Wakino, Y. Tanabe, et al., Rho and Rho-kinase activity in adipocytes contributes to a vicious cycle in obesity that may involve mechanical stretch, Sci. Signal 4 (2011), https://doi.org/10.1126/scisignal.2001227 ra3.

[8] K. Bhadriraju, M. Yang, S. Alom Ruiz, et al., Activation of ROCK by RhoA is regulated by cell adhesion, shape, and cytoskeletal tension, Exp. Cell Res 313 (2007) 3616–3623, https://doi.org/10.1016/j.yexcr.2007.07.002.

[9] M.A. Wozniak, R. Desai, P.A. Solski, et al., ROCK-generated contractility regulates breast epithelial cell differentiation in response to the physical properties of a three-dimensional collagen matrix, J. Cell Biol 163 (2003) 583–595, https://doi.org/10.1083/jcb.200305010.

[10] M.N. Andalib, J.S. Lee, L. Ha, et al., The role of RhoA kinase (ROCK) in cell alignment on nanofibers, Acta Biomater 9 (2013) 7737–7745, https://doi.org/10.1016/j.actbio.2013.04.013.

[11] M. Spencer, A. Yao-Borengasser, R. Unal R, et al., Adipose tissue macrophages in insulin-resistant subjects are associated with collagen VI and fibrosis and demonstrate alternative activation, Am. J. Physiol. Endocrinol. Metab. 299 (2010) E1016–E1027, https://doi.org/10.1152/ajpendo.00329.2010.

[12] C. Henegar, J. Tordjman, V. Achard, et al., Adipose tissue transcriptomic signature highlights the pathological relevance of extracellular matrix in human obesity, Genome Biol 9 (2008) 1–32, https://doi.org/10.1186/gb-2008-9-1-r14.

[13] E.M. Darling, M. Topel, S. Zauscher, et al., Viscoelastic properties of human mesenchymally-derived stem cells and primary osteoblasts, chondrocytes, and adipocytes, J. Biomech. 41 (2008) 454–464, https://doi.org/10.1016/j.jbiomech.2007.06.019.

[14] Y.N. Kwon, W.K. Kim, S.H. Lee, et al., Monitoring of adipogenic differentiation at the single-cell level using atomic force microscopic analysis, Spectroscopy 26 (2011) 329–335, https://doi.org/10.1155/2011/707216.

[15] J.S. Lee, L. Ha, J.H. Park, et al., Mechanical stretch suppresses BMP4 induction of stem cell adipogenesis via upregulating ERK but not through downregulating Smad or p38, Biochem. Biophys. Res. Commun. 418 (2012) 278–283, https://doi.org/10.1016/j.bbrc.2012.01.010.

[16] Q. Tseng, E. Duchemin-Pelletier, A. Deshiere, et al., Spatial organization of the extracellular matrix regulates cell-cell junction positioning, Proc. Natl. Acad. Sci. U. S. A. 109 (2012) 1506–1511, https://doi.org/10.1073/pnas.1106377109.

[17] M.H. Yen, Y.H. Chen, Y.S. Liu, et al., Alteration of Young's modulus in mesenchymal stromal cells during osteogenesis measured by atomic force microscopy, Biochem. Biophys. Res. Commun. 526 (2020) 827–832, https://doi.org/10.1016/j.bbrc.2020.03.146.

[18] B.D. Riehl, E. Kim, T. Bouzid, et al., The role of microenvironmental cues and mechanical loading milieus in breast cancer cell progression and metastasis, Front. Bioeng. Biotechnol. 8 (2021) 1571, https://doi.org/10.3389/fbioe.2020.608526.

[19] C. Huang, J. Dai, X.A. Zhang, Environmental physical cues determine the lineage specification of mesenchymal stem cells, Biochim. Biophys. Acta 1850 (2015) 1261–1266, https://doi.org/10.1016/j.bbagen.2015.02.011.

[20] S. Or-Tzadikario, A. Gefen, Confocal-based cell-specific finite element modeling extended to study variable cell shapes and intracellular structures: the example of the adipocyte, J. Biomech. 44 (2011) 567–573, https://doi.org/10.1016/j.jbiomech.2010.09.012.

[21] A.R. Saltiel, J.M. Olefsky, Inflammatory mechanisms linking obesity and metabolic disease, J. Clin. Invest. 127 (2017) 1–4, https://doi.org/10.1172/JCI92035.

[22] E.K. Dimitriadis, F. Horkay, J. Maresca, et al., Determination of elastic moduli of thin layers of soft material using the atomic force microscope, Biophys. J. 82 (2002) 2798–2810, https://doi.org/10.1016/S0006-3495(02)75620-8.

[23] J.C. Hansen, J.Y. Lim, L.C. Xu, et al., Effect of surface nanoscale topography on elastic modulus of individual osteoblastic cells as determined by atomic force microscopy, J. Biomech. 40 (2007) 2865–2871, https://doi.org/10.1016/j.jbiomech.2007.03.018.

[24] B.D. Pope, C.R. Warren, K.K. Parker, et al., Microenvironmental control of adipocyte fate and function, Trends Cell Biol. 26 (2016) 745–755, https://doi.org/10.1016/j.tcb.2016.05.005.

[25] J.K. Wenderott, C.G. Flesher, N.A. Baker, et al., Elucidating nanoscale mechanical properties of diabetic human adipose tissue using atomic force microscopy, Sci. Rep. 10 (2020) 1–9, https://doi.org/10.1038/s41598-020-77498-w.

[26] K. Sun, J. Tordjman, K. Clément, et al., Fibrosis and adipose tissue dysfunction, Cell Metabol. 18 (2013) 470–477, https://doi.org/10.1016/j.cmet.2013.06.016.

[27] K. Sun, C.M. Kusminski, P.E. Scherer, Adipose tissue remodeling and obesity, J. Clin. Invest. 121 (2011) 2094–2101, https://doi.org/10.1172/JCI45887.

[28] M. Amano, M. Ito, K. Kimura, et al., Phosphorylation and activation of myosin by Rho-associated kinase (Rho-kinase), J. Biol. Chem. 271 (1996) 20246–20249, https://doi.org/10.1074/jbc.271.34.20246.

[29] B.D. Riehl, J.S. Lee, L. Ha, et al., Flowtaxis of osteoblast migration under fluid shear and the effect of RhoA kinase silencing, PLoS One 12 (2017), e0171857, https://doi.org/10.1371/journal.pone.0171857.

[30] P.K. Chaudhuri, C.Q. Pan, B.C. Low, et al., Topography induces differential sensitivity on cancer cell proliferation via Rho-ROCK-Myosin contractility, Sci. Rep. 6 (2016) 1–9, https://doi.org/10.1038/srep19672.

[31] L. Hyväri, M. Ojansivu, M. Juntunen, et al., Focal adhesion kinase and ROCK signaling are switch-like regulators of human adipose stem cell differentiation towards osteogenic and adipogenic lineages, Stem Cell. Int. 2018 (2018) 2190657, https://doi.org/10.1155/2018/2190657.